

Transient backbending behavior in the Ising model with fixed magnetizationF. Gulminelli,¹ J. M. Carmona,² Ph. Chomaz,³ J. Richert,⁴ S. Jiménez,⁵ and V. Regnard^{1,3}¹*LPC Caen (IN2P3-CNRS/ISMRA et Université), F-14050 Caen Cédex, France*²*Departamento de Física Teórica, Universidad de Zaragoza, 50009 Zaragoza, Spain*³*GANIL (DSM-CEA/IN2P3-CNRS), Boîte Postale 5027, F-14076 Caen Cédex 5, France*⁴*Laboratoire de Physique Théorique (UMR7085), Université Louis Pasteur, 3 rue de l'Université, 67084 Strasbourg Cédex, France*⁵*Departamento de Física Teórica, Universidad de Zaragoza, 50009 Zaragoza, Spain*

(Received 10 February 2003; revised manuscript received 23 May 2003; published 20 August 2003)

The physical origin of the backbendings in the equations of state of finite but not necessarily small systems is studied in the Ising model with fixed magnetization (IMFM) by means of the topological properties of the observable distributions and the analysis of the largest cluster with increasing lattice size. Looking at the convexity anomalies of the IMFM thermodynamic potential, it is shown that the order of the transition at the thermodynamic limit can be recognized in finite systems independently of the lattice size. General statistical mechanics arguments and analytical calculations suggest that the backbending in the caloric curve is a transient behavior which should not converge to a plateau in the thermodynamic limit, while the first-order transition (in the Ehrenfest sense) is still signaled by a discontinuity in the magnetization equation of state.

DOI: 10.1103/PhysRevE.68.026119

PACS number(s): 05.50.+q, 64.10.+h, 68.03.Cd, 05.70.Fh

I. INTRODUCTION

The origin of singularities in thermodynamic functions which characterize infinite systems undergoing phase transitions is a central issue in statistical mechanics. However, physical systems are finite. It is therefore necessary to introduce specific tools which allow to detect and characterize these singularities in the corresponding finite systems. A possible approach deals with the distribution of zeroes of the partition sum in the complex temperature plane [1]. Alternatively, it has been observed that nonanalyticities can originate from a backbending in an equation of state corresponding to an anomalous curvature of the thermodynamic potential surface [2]. In particular, a convex intruder in the microcanonical entropy leading to a backbending in the functional relationship between temperature and energy (caloric curve) has been proposed as a general definition of first-order phase transitions in finite systems [3]. Indeed, negative heat capacities have been observed and connected to first-order phase transitions in different models [4–6] and even experimentally measured [7–9].

In this context, the Ising model with fixed magnetization (IMFM) presents some very peculiar features. For small systems, the microcanonical caloric curve which relates energy to temperature does not show any backbending in the temperature domain where a first-order phase transition exists in the Ising model [10]. This finding shows that backbendings are deeply connected to the constraints which are imposed on the system [10,11] and their presence may depend on the physical quantities which are used in order to define the considered statistical ensemble as it will be shown later [12]. It is well known that IMFM is isomorphous to an isochore lattice gas model. If we consider that no divergence is expected for the heat capacity at constant volume in the macroscopic liquid to gas phase transition, the absence of a backbending in the microcanonical caloric curve illustrates the fact that there may be no one to one correspondence between first-order phase transitions and convexity anomalies of the

microcanonical entropy as a function of energy. This seems to be confirmed by recent analytic arguments [14] which lead to the conclusion that the transition is continuous, in the sense that the caloric curve has no plateau in the thermodynamic limit. However, according to Ref. [13], a backbending appears in the caloric curve of very large lattices. The thermodynamic limit of this behavior is not clear in view of the present status of Monte Carlo simulations. Moreover, the cluster properties of small IMFM lattices show different signs of critical behavior [15]. Together with the information coming from the caloric curve, this could suggest that the apparent order of the transition in the IMFM model changes with the size of the system.

In the present paper, we shall try to clarify these issues by using a definition of phase transitions based on the occurrence of bimodalities in the probability distribution of an observable [16]. This definition is a generalization of the one based on curvature anomalies and satisfies the Yang Lee unit circle theorem in the thermodynamic limit [16,17]. Since, in Gibbs equilibria, a bimodal distribution of an observable is connected to the backbending of the associated equation of state in the ensemble where the observable is constrained by a conservation law, this study will allow us to elucidate the relationship between backbendings, constraints, and the order of the transition.

We shall first analyze the topology of the events in the Ising model (Sec. II) to show that many properties of IMFM can be understood starting from the standard Ising model. We shall see that backbendings are not characteristic of the caloric curve only but can appear in other equations of state also and closely depend on the constraints applied to the system, i.e., on the statistical ensemble in which the system is studied. In Sec. III, we shall consider the behavior of the IMFM and see that for all sizes, the transition can be unambiguously recognized as a first order transition even if a backbending appears in the microcanonical caloric curve only for large sizes and may disappear at the thermodynamic limit. Concerning this limit, a first-order transition does not

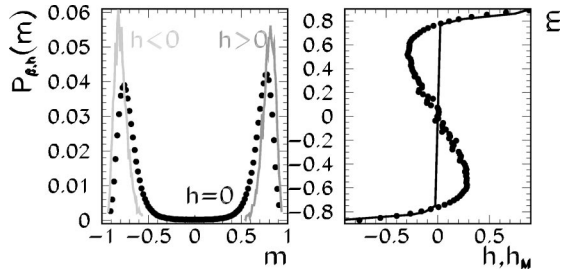


FIG. 1. Ising calculation of an $L=6$ cubic lattice with periodic boundary conditions at a subcritical temperature $T < T_c$. Left side: magnetization distribution with a negative, zero, and positive external fields. Right side: (full line) average magnetization as a function of the external field; (symbols) field h_M in the IMFM model obtained by derivation of the magnetization distribution at zero field [see Eq. (5)].

imply the convergence of the backbending to a finite energy jump. Some general arguments for a zero energy discontinuity will be given in Sec. IV and complemented by a study of cluster properties. In order to confirm the outcome of the numerical simulations, an analytical model of a finite system with negative heat capacity converging to a caloric curve, which does not show a plateau in the thermodynamic limit even if the system is undergoing a first-order phase transition, will be given in Sec. V.

II. TOPOLOGY OF EVENTS IN THE ISING MODEL

We shall first concentrate on the well known Ising model to show that the topologic properties of observable distributions [16] allow us to get some hint about the behavior of the IMFM model.

The order parameter of the standard Ising model is the magnetization $M = \sum_i s_i$, where $s_i = \pm 1$ and the sum extends to the N sites of a lattice. It is interesting to note that because of the mapping between the Ising model and the Lattice Gas model $s_i = 2n_i - 1$, a spin up $s_i = 1$ can also be interpreted as an occupied site $n_i = 1$. Then, the magnetization is mapped into the order parameter for the Lattice Gas model, which is nothing but the number of particles $A = \sum_i n_i$. Since the volume is fixed, A indeed corresponds to the density $\rho = A/N$, the known order parameter of the liquid-gas phase transition. We shall also use the average magnetization per site $m = M/N$ which is then isomorphous to a particle density via $m = 2\rho - 1$. In the Ising model, neighboring sites interact via a constant attractive coupling $\epsilon < 0$. In our numerical implementations of the model we have considered three-dimensional cubic lattices characterized by a linear dimension $L = N^{1/3}$ with periodic boundary conditions. Details about the Metropolis simulations can be found in Ref. [18].

Below the critical temperature T_c , the Ising model shows a first-order phase transition at zero field $h=0$ which is characterized, in infinite systems, by a discontinuity of the magnetization when the field changes sign. This jump is clearly visible in the standard average magnetization versus field equation of state already for a lattice as small as $L=6$ as shown in the right part of Fig. 1. The transition from the dominantly negative to the dominantly positive solution

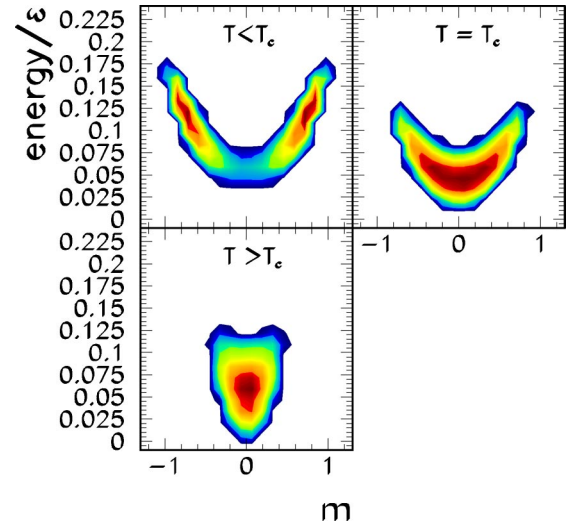


FIG. 2. (Color online) Magnetization versus energy distributions with a zero external field for an $L=6$ Ising lattice at different temperatures.

passes through a bimodality of the magnetization distribution, shown in the left part of Fig. 1, which can be taken as a definition of phase coexistence, the two peaks being associated with the two phases [16,17,19]. The transition field is the one for which the two peaks have the same height so that the most probable magnetization jumps from negative to positive values. For symmetry reasons, this, of course, occurs at $h=0$. The intuitive understanding of phase coexistence given by this topological definition is clearly seen in Fig. 2 which gives the magnetization distribution as a function of temperature, for the same $L=6$ lattice at $h=0$ field. At supercritical temperatures the distributions are normal while the critical point can be seen as a bifurcation point from which the distribution splits into two separated components or phases.

It is important to note that a bimodality in the distribution of an observable implies a backbending for the associated equation of state in the statistical ensemble where this observable is controlled on an event by event basis. Let us see this in the case of the Ising model with a magnetic field (grand canonical ensemble), with partition function

$$Z_{\beta h} = \sum_{E, M} W(E, M) e^{-\beta(E - hM)}, \quad (1)$$

where $\beta = T^{-1}$ and $W(E, M)$ is the number of configurations or microstates with energy E and magnetization M , and the Ising model with fixed magnetization M (canonical ensemble), with partition function

$$Z_{\beta}(M) = \sum_E W(E, M) e^{-\beta E}. \quad (2)$$

The two partition functions are related by

$$Z_{\beta h} = \sum_M Z_{\beta}(M) e^{(\beta h M)}. \quad (3)$$

The magnetization distribution of the Ising model reads

$$p_{\beta h}(M) = \frac{1}{Z_{\beta h}} \sum_E W(E, M) e^{-\beta(E-hM)} = \frac{Z_{\beta}(M)}{Z_{\beta h}} e^{(\beta h M)}. \quad (4)$$

This equation shows that the magnetization distribution $p_{\beta h}(M)$ in the standard Ising can be directly related to the partition sum of the IMFM. The thermodynamic relations for the IMFM can thus at least, in principle, be calculated from $p_{\beta h}(M)$ without a direct simulation of the IMFM [29]. In particular, the equation of state related to the magnetization in the IMFM reads

$$h_M \equiv -\frac{1}{\beta} \frac{\partial \ln Z_{\beta}(M)}{\partial M} = -\frac{1}{\beta} \frac{\partial \ln p_{\beta h}(M)}{\partial M} + h. \quad (5)$$

Equation (5) shows that a bimodality in $p_{\beta h}(M)$ implies a backbending of the intensive parameter h_M (which has the dimension of a magnetic field) associated with the magnetization as shown on the right-hand side of Fig. 1. It is important to stress that h_M is not a mathematical artifact. Outside the coexistence region, it represents the physical magnetic field which, applied to Ising, gives M as the most probable response. Indeed, in the presence of an external field h , the most probable magnetization should fulfill

$$\frac{\partial \ln p_{\beta h}(M)}{\partial M} = \frac{\partial \ln Z_{\beta}(M)}{\partial M} + \beta h = \beta(h - h_M) = 0, \quad (6)$$

i.e., the (most probable) response is M if the applied field is $h = h_M$. This is true as long as the system is not undergoing a phase transition, i.e., as long as Eq. (6) has only one solution. Indeed, Eq. (6) defines the extrema of the probability distribution. When the solution is unique this unique extremum can only be a maximum. In the transition regions, i.e., in the backbending region, Eq. (6) has three solutions, two maxima and a minimum in between. This corresponds to the subcritical temperatures for which $p_{\beta h}(M)$ is bimodal in a region around $h=0$. In this regime, the interval Δh_M associated with the backbending corresponds exactly to the interval Δh for which $p_{\beta h}(M)$ is bimodal. The values of (E, M) inside the coexistence region are not equilibrium states in the Ising model with magnetic field: the only physical ensemble for experiments exploring coexistence is the IMFM and in this case h_M (and not h) is the real physical conjugate to the magnetization [7–9].

This discussion can be immediately extended to any generic Gibbs equilibrium [16]. A phase coexistence (first-order phase transition) is signaled by a bimodality in the probability distribution of an extensive variable which can then be identified as an order parameter. This topological anomaly is equivalent to a convexity anomaly in the thermodynamic potential of the ensemble in which the order parameter is constrained by a conservation law (extensive ensemble), and reflects in a backbending of the associated intensive variable in this extensive ensemble. A backbending in the order parameter equation of state is an alternative possible definition of a first-order phase transition in an extensive ensemble of a finite system [3].

In particular, the bimodality of the magnetization distribution observed for the standard Ising model with no constraints on the magnetization ($h=0$) at subcritical temperatures (Fig. 2) implies that the magnetic susceptibility of IMFM is negative for magnetization domains lying between the two dominant peaks of Ising. This negative susceptibility, analogously to a negative heat capacity in a microcanonical ensemble, indicates a first order phase transition. The connection between the bimodality of the magnetization distribution and a negative susceptibility is valid for all finite sizes up to the thermodynamic limit. Therefore, the well-known fact that the Ising bimodality converges to a finite jump in the thermodynamic limit guarantees that the corresponding phase transition in IMFM is also first-order up to the thermodynamic limit. This situation is analogous to the relationship between the grandcanonical and the canonical ensembles discussed in the context of the Yang-Lee theorems [20].

In the recent literature of phase transitions in finite systems [3], backbendings have been often observed in the microcanonical caloric curve, leading to negative heat capacity. Following the general relationship between ensembles discussed above, a negative heat capacity univocally implies a bimodal energy distribution in the corresponding canonical ensemble. Figure 2 shows that because of the symmetry between spins up and down in the Ising Hamiltonian, the two magnetization solutions correspond to the same energy. This means that the energy cannot be used as an order parameter for this model. On the other hand, all variables correlated to the magnetization can present a bimodality, i.e., can be considered as order parameters. As an example, Fig. 3 shows the correlation between the magnetization and the size of the largest connected domain A_{max} , here defined with the Coniglio-Klein algorithm [21] in its simplified version proposed by Campi and Krivine [22].

III. THE IMFM AND THE EFFECT OF CONSTRAINTS

In the preceding section, we have recalled that an order parameter of a first-order phase transition can be defined as any observable O which allows us to separate the two phases, i.e., such that if events are sorted as a function of O , they split into two components separated by a minimum of the distribution function. This definition is valid only if the order parameter is free to fluctuate (i.e., in the Ising model). If the order parameter is constrained by a conservation law (i.e., in the IMFM), the first-order character of the transition can still be recognized from the backbending of the equation of state relating the order parameter to its conjugate intensive variable. In the case of the IMFM, this would require to calculate the derivatives of the partition sum for all values of the magnetization. However, because of the exact equivalence between bimodalities in the intensive ensemble and backbendings in the extensive one (see Sec. II), the direct simulation of the IMFM with different magnetizations is not necessary. A single Ising calculation of the energy and magnetization distribution is sufficient to completely identify the coexistence zone of IMFM and recognize the first-order character of the transition.

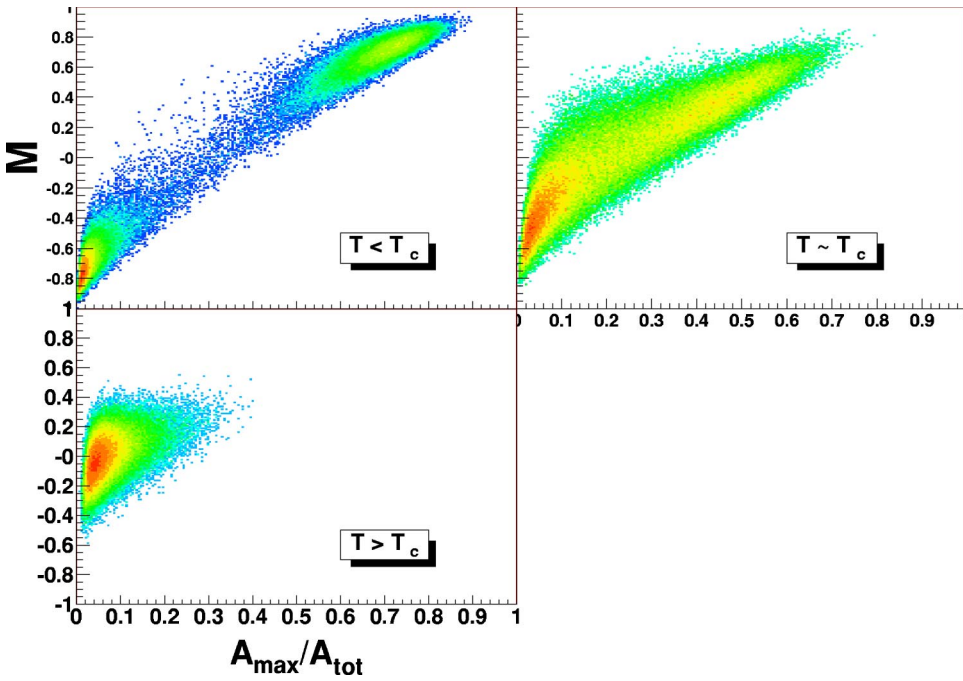


FIG. 3. (Color online) Correlation between magnetization and the size of the largest connected domain for an $L=6$ Ising lattice with zero field at three different temperatures $T=4\epsilon, 4.8\epsilon, 7.2\epsilon$.

In the general case, bimodalities have not to be expected in models such as IMFM where the order parameter is fixed by a conservation law (see, however, Refs. [23,24] for an exception). However, in the case of finite systems, fluctuations are not negligible and the relationship between M and A_{max} is not a one to one correspondence but rather a loose correlation. This implies that for finite systems, a bimodality in the A_{max} distribution can remain even in the constant magnetization ensemble. This is shown in Fig. 4, which displays the A_{max} distribution for the IMFM with a number $A=60$ of positive spins (or lattice gas particles) in a $L=20$ cubic lattice (corresponding to a magnetization $m=M/N=-0.985$ and a low density $\rho=0.0075$) at a temperature $T=T_{tr}$ where

T_{tr} corresponds to the transition temperature, i.e., the temperature at which the two maxima of the energy distribution have the same height. As shown in Fig. 5 (left), A_{max} is correlated with the energy E , so that the bimodality in A_{max} reflects in a bimodality in the energy distribution. The bimodality in the energy distribution implies that the microcanonical IMFM caloric curve presents a backbending. We have just interpreted this backbending as a finite-size effect (and we shall come back to this point in the following section). However, for very small systems, this behavior is not visible. This is shown in the right parts of Figs. 4 and 5 below, in agreement with the results of Ref. [13]. In the upper right part of Fig. 5, the same system of $A=60$ positive spins now occupies an $L=5$ lattice, corresponding to a magnetization

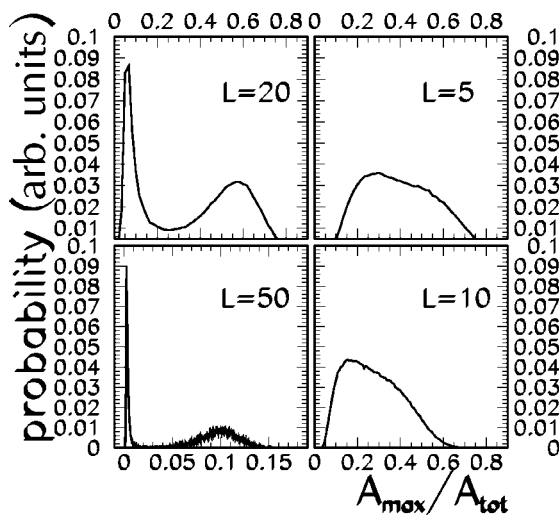


FIG. 4. IMFM largest connected domain distribution for (upper part) lattice sizes $L=20$ and $L=5$ with the same $A=60$ number of positive spins; (lower part) lattice sizes $L=50$ and $L=10$ with the same density of positive spins $\rho=0.13$ (same magnetization $m_0=-0.74$).

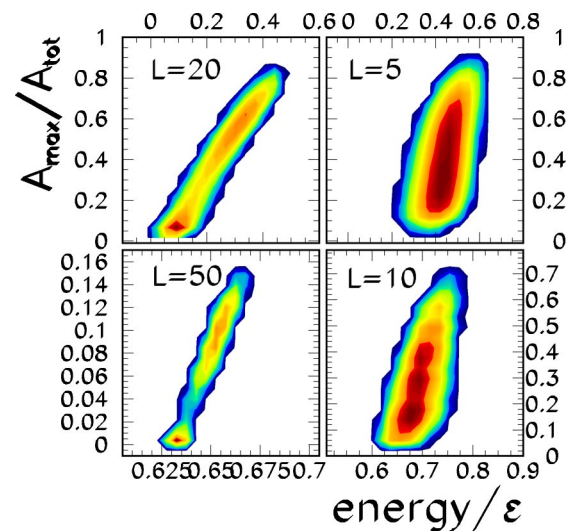


FIG. 5. (Color online) A_{max} versus energy correlations for (upper part) an $A=60$ system in an $L=20$ and $L=5$ lattices; (lower part) a $\rho=0.13$ system in $L=50$ and $L=10$ lattices.

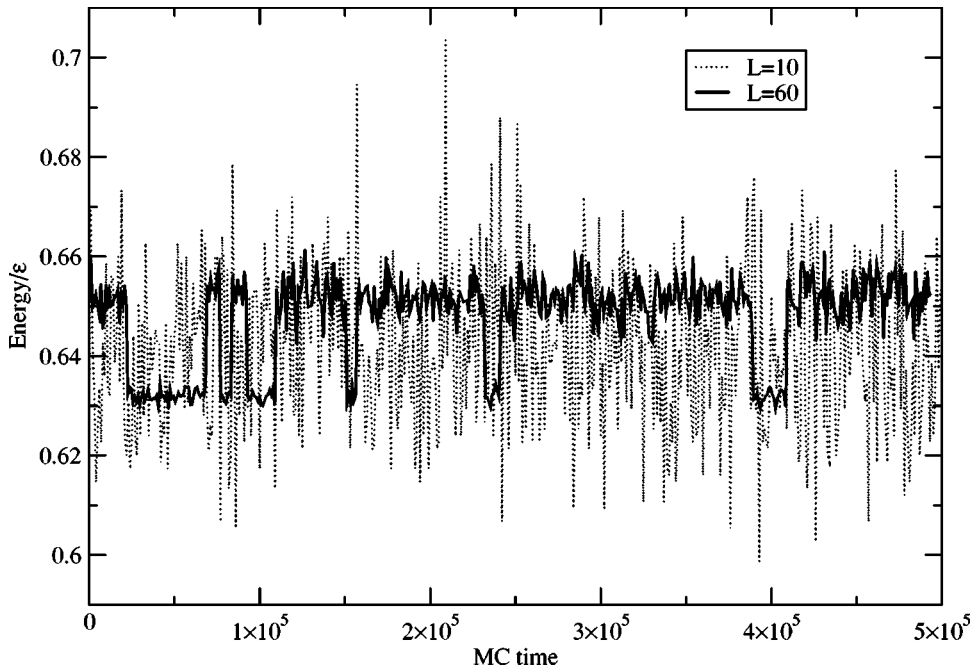


FIG. 6. Total energy as a function of the Metropolis step for $m = 0.75$ and lattices of linear sizes $L = 10$ and $L = 60$ at the transition temperature.

$m = -0.04$ (or a density $\rho = 0.48$). The calculation has been done at a temperature such that the average energy $\langle E \rangle$ is the same as in the $L = 20$ case, to be sure that the expected region of the backbending is explored. The A_{max} as well as the E distributions are monomodal, and no bimodality is ever seen for any value of T in this small lattice. The fact that this is correlated to a finite-size effect is demonstrated in the lower part of Fig. 5, where the same trend is observed keeping the reduced magnetization constant and varying only the size of the lattice.

This behavior can be understood because the correlation between A_{max} (and so the energy) and M becomes looser the smaller the size of the system. For very small systems, the width of the two peaks becomes comparable to their distance and the bimodality cannot be seen any more.

An intuitive understanding of this phenomenon can be obtained looking at Fig. 6, which gives the total energy as a function of the Metropolis steps for two systems, $L = 10$ and $L = 60$, at the same density $\rho = 0.13$. The width of the distribution is comparable for the two lattice sizes (the energy jump evolves slowly with L [13]), but in the small lattice the large fluctuations around each solution do not allow us to resolve the two peaks [25].

Recalling that the two Ising phases are exactly degenerate in energy (see Fig. 2), one can wonder whether the two “phases” visible in Fig. 5 have some relationship with Ising phases at all. Indeed, Fig. 5 could rather suggest that we are studying a different (temperature driven) phase transition between an ordered and a disordered phase which has nothing to do with the Ising phase transition driven by the magnetic field. This is however not possible. Indeed, Ising and IMFM correspond to the same Hamiltonian and only differ because of the constraints. Equations (2)–(4) guarantee that for every finite system, whatever its size, the two models explore the very same density of states $W(E, M)$ with different weights, i.e., share the same phase diagram.

The situation can be clarified if we look at Fig. 7 which shows the correlation between energy and the mean cubic radius of the system defined as

$$V = \frac{4}{3} \frac{\pi}{A} \sum_{i=1}^N r_i^3 \frac{s_i + 1}{2}, \quad (7)$$

where r_i is the distance from the center of mass of the lattice. Figure 7 shows that the two different energy solutions or phases which give the energy bimodality in the IMFM correspond to very different spatial extensions. As a consequence, the two peaks in Figs. 5 and 7 can be related to the two Ising solutions (see Fig. 2) in a three-dimensional space that has volume as an extra dimension.

Indeed, in the liquid-gas universality class, the order parameter is particle density. A bimodal particle density distribution can be obtained if the volume is fixed and the particle number is free to fluctuate (as in the Ising model) or if the particle number is fixed and the volume is free to fluctuate (as in the isobar lattice gas model [4]). In the isochore canonical case represented by the IMFM, the two configurations corresponding to the two different phases cannot, in general, be explored because of the boundary condition con-

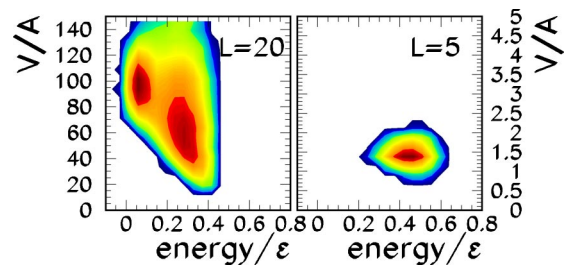


FIG. 7. (Color online) Volume (see text) versus energy correlations for $A = 60$ IMFM system in an $L = 20$ and $L = 5$ lattices.

straint as it can be seen in the right part of Fig. 7. There is, however, an exception to this statement. If the number of minority spins or particles grows slower than the available volume such that $A/L^3 \rightarrow 0$, the boundary conditions will not be felt by the system. Going towards this limit, a single calculation with a given lattice size L_0 can give rise to both compact events (typical of the positive magnetization Ising phase for a smaller $L < L_0$ lattice at the same temperature) and rarified events (typical of the negative magnetization Ising phase in a larger $L > L_0$ lattice). This is the situation depicted in the left part of Figs. 5 and 7, and studied at length in Ref. [13]. The energy bimodality in the IMFM for the lattice size L_0 is then a reflection of the high-density and low-density phases of the Ising model corresponding to lattice sizes which are smaller and higher, respectively, than L_0 . In the “true” thermodynamic limit $A/L^3 \rightarrow \text{const}$, we expect this bimodality to disappear as we will see in the following section.

IV. SIZE DISTRIBUTIONS AND THE THERMODYNAMIC LIMIT

We have just shown that for (not too) small systems, the energy distribution of the IMFM can be bimodal. A systematic study of this phenomenon can be found in Ref. [13]. If this bimodality (or, equivalently, backbending of the micro-canonical caloric curve) would survive up to the thermodynamic limit, at the canonical temperature T_{tr} at which the two peaks have the same height, one would observe at the thermodynamic limit a jump in the average energy from the disordered to the ordered phase. T_{tr} would then be the transition temperature of a conventional first-order phase transition with a finite latent heat. In Sec. III, we have noticed that the bimodality in energy is correlated to a bimodality in A_{max} , therefore an indication about the thermodynamic limit of the energy distribution can be obtained from an inspection of the size distribution.

Figure 8 shows the distributions of fragment sizes at the fixed magnetization density $m = -0.5$. The corresponding phase diagram is reported in Fig. 9 [2]. At a given lattice size, a two-parameter power-law fit has been performed for each temperature; the temperature at which the χ^2 of the fit is minimum is then defined as the “critical” temperature and reported in Fig. 9 as a dashed line (for $L=8$) and as a dotted line (for $L=50$) [2]. A first-order transition is clearly indicated in the bigger lattice calculation. At a temperature slightly lower than T_c (lower left panel of Fig. 8 and lower horizontal line in Fig. 9), the “infinite” percolation cluster is still present. At a temperature slightly higher than T_c (lower right panel of Fig. 8 and higher horizontal line in Fig. 9), the infinite percolation cluster has disappeared. As it can be seen from Fig. 8, the disappearance point of the percolation cluster does not correspond to a power law (and, in fact, finite-size scaling of the cluster size distributions is violated on the dotted line up to the critical point [2]). Similar results have also been presented in Ref. [15]. In the case of very small lattices, the percolation cluster is so small that its size is comparable to the size of the other fragments; this creates an apparent and transient power-law behavior in the middle of

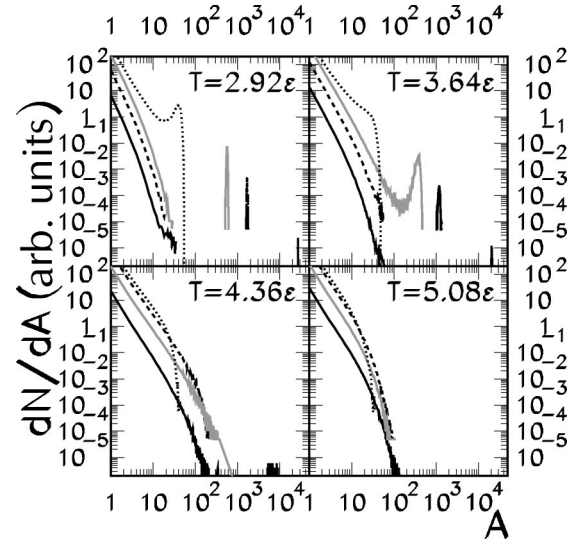


FIG. 8. Distribution of cluster size in the IMFM at four different temperatures and a fixed magnetization density $m = -0.5$ for cubic lattices of linear dimension $L = 50$ (black), $L = 20$ (dashed), $L = 14$ (gray), and $L = 8$ (dotted).

the coexistence zone [2], which is a finite-size effect which should not be confused with a continuous transition. The sudden disappearance of the percolation cluster suggests a finite jump, in the distribution of A_{max} at the transition temperature in the thermodynamic limit, and consequently a finite latent heat. For the results of Fig. 8 to be compatible with zero energy jump it is however enough that the size of the largest cluster increases more slowly than L^3 with increasing lattice size.

From a conceptual point of view, we do not expect that the bimodality of the A_{max} distribution or equivalently the backbending of the caloric curve converges to a discontinuity at the thermodynamic limit. Indeed the Van Hove theorem

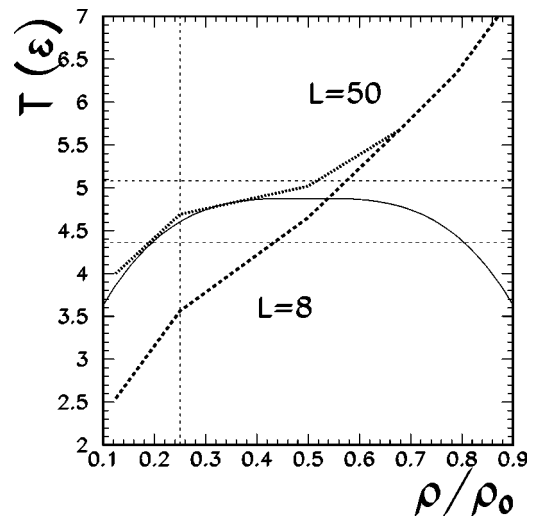


FIG. 9. Phase diagram of the IMFM with periodic boundary conditions. Full line: coexistence line from Refs. [2]; dashed (dotted) line: curve of the minimum chi-square two-parameter fit of the size distribution with a power law for $L = 8$ ($L = 50$).

TABLE I. Transition temperatures and difference between the two (intensive) energy values of the peaks present in the energy histogram of several lattice sizes between $L=42$ and $L=60$ at $\rho=0.13$.

L	$T_{tr}(\epsilon)$	$\Delta E/\epsilon$
42	3.807(1)	0.0219(1)
46	3.824(1)	0.0216(2)
50	3.838(1)	0.0212(1)
54	3.851(1)	0.0210(1)
60	3.866(1)	0.0200(2)

[20] guarantees, for short-range forces, the equivalence of the ensembles at the thermodynamic limit. Therefore, the IMFM equations of state should converge to the Ising ones even in the coexistence region of first-order phase transitions. Moreover, the Ising model belongs to the liquid-gas universality class (the IMFM is, in fact, isomorphous to the canonical lattice-gas model at constant volume) and this implies that the IMFM at the thermodynamic limit should be equivalent to the macroscopic liquid-gas phase transition at a constant volume which exhibits a continuous caloric curve with no energy jump at a constant temperature. This agrees with the findings of Ref. [14] and remarks that a continuous behavior of the energy is compatible with a first-order transition.

On the other hand, if one constructs a lattice gas model at a fixed pressure [4], the backbending in the energy is visible even for very small lattice sizes and should converge to a plateau in the thermodynamic limit. The constant volume and constant pressure situations are the same in the particular case of zero pressure which corresponds to an infinite volume independent of the number of particles (i.e., of the magnetization M). Since the infinite volume is a constant pressure situation, a backbending is expected for the microcanonical caloric curve of the finite system in an infinite volume, i.e., for a density going to zero. This is indeed what is observed in Fig. 5 above. The left side of Fig. 5 can be interpreted in this context as a calculation at constant (low) pressure, such that the spatial extension of the system is not constrained by any boundary conditions ($N \rightarrow \infty$). Within this interpretation, it is natural that the backbendings observed in Ref. [13] appear for large lattice sizes compared to the number of particles. Going towards the thermodynamic limit, however, the isobar and isochore paths correspond to different physical situations and an energy jump should be associated only with a transformation at a constant pressure.

The transient nature of the bimodality can be, in principle, directly demonstrated looking at the distance between the two energy peaks at the transition temperature (energy jump) [13] at a fixed magnetization as a function of the lattice size. Table I shows the magnitude of the energy jump between the two peaks for several lattices between $L=42$ and $L=60$ at $\rho=0.13$. This calculation is excessively delicate. Indeed, the transition region in large lattices is very narrow, and the bimodality is only seen in a very short range of T ($\Delta T \sim 10^{-3}\epsilon$ for $L=60$). The transition temperature is then ob-

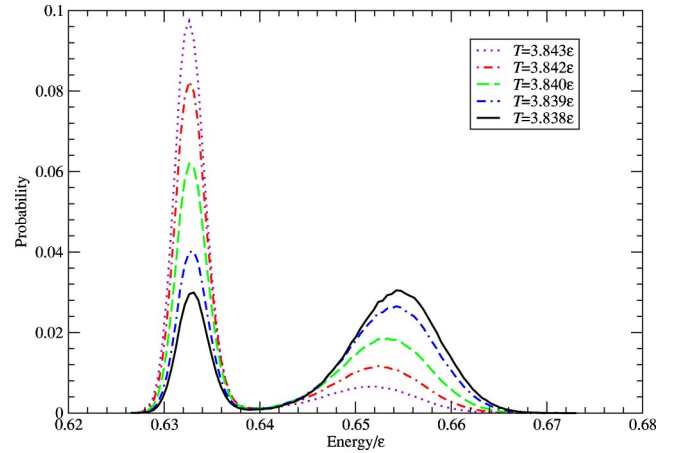


FIG. 10. (Color online) Ferrenberg-Swendsen calculation of energy histograms for an $L=50$ lattice at $\rho=0.13$. T_{tr} is found to be 3.838ϵ .

tained by a Ferrenberg-Swendsen algorithm [26], which moves the energy histograms found at a certain T at which the bimodality is present and finds the T_{tr} at which both peaks have the same height. Figure 10 illustrates this procedure.

The results of Table I show a tendency of the distance between the peaks to decrease, although very slowly. Extending this study to larger lattices is a very hard computational task. Apart from the increase in computer time of Monte Carlo steps ($\propto L$), when L is very large, the Monte Carlo time between jumps increases too, what makes very difficult to perform the Ferrenberg-Swendsen analysis described above. For the moment, making this analysis for lattice sizes $L > 60$ lies beyond the possibilities of our present computers.

V. AN ANALYTICAL MODEL

The fact that energy can play the role of an order parameter in the IMFM, as well as its transient character, has been up to now discussed in the framework of numerical simulations. Whatever the numerical procedure, the quality of the exploration of the phase space becomes increasingly delicate with increasing number of possible configurations, i.e., size of the lattice. In this section, we shall therefore make use of the fact that Ising belongs to the liquid-gas universality class to show in a simple analytical liquid drop model that (1) the microcanonical caloric curve can backbend at constant volume; (2) this backbending disappears at the thermodynamic limit; (3) the convergence can be very slow and it is not surprising that an apparent energy jump still survives for lattice sizes as large as $L=50$.

Let us consider a liquid-gas phase coexistence as a spherical liquid drop in equilibrium with an ideal gas of monomers [27]. This picture will not apply to very small systems (for which the liquid drop approximation as well as the monomer approximation will fail), while the thermodynamic limit will be recovered by letting the droplet radius $R \rightarrow \infty$. The equilibrium between the droplet and the vapor can be obtained by equalizing the chemical potential of the two phases which leads to the Clapeyron equation

$$\frac{dp}{dT} = \frac{\Delta s}{\Delta v} = \frac{\Delta e + p\Delta v}{T\Delta v}, \quad (8)$$

which expresses the relation between the pressure p and temperature T in the coexistence zone of the first-order phase transition. Here, Δs , Δv , Δe represent the difference in entropy, volume and energy per particle between the two phases. In the low pressure regime, the liquid specific volume v_l is much lower than the gas specific volume, $v_l \ll v_g$, and the vapor can be considered as an ideal gas of monomers $pv_g = T$ leading to [28]

$$\frac{dp}{dT} = \frac{(\Delta e + T)p}{T^2}. \quad (9)$$

If, in addition we consider the subcritical regime where the temperature is much lower than the typical latent heat $T \ll \Delta e$, we can consider the latent heat as a constant, i.e., $\Delta e(p, T) \approx \text{const}$, and the Clapeyron equation is readily integrated giving

$$p = p_0 \exp\left(-\frac{\Delta e}{T}\right). \quad (10)$$

If the liquid fraction is constituted by a finite drop, its binding energy per particle Δe is reduced with respect to its bulk value Δe_0 [27], $\Delta e = \Delta e_0 - 3a_s v_l / R$ where a_s is the surface energy coefficient and $R = r_0 A^{1/3}$ is the drop radius. The equality between the liquid pressure Eq. (10) and the vapor pressure $p = T/v_g$ gives

$$p_0 \exp\left(-\frac{\Delta e_0}{T} + \frac{3a_s v_l}{r_0 A^{1/3} T}\right) = \frac{T(A_{tot} - A)}{V - A v_l}, \quad (11)$$

where A is the mass number of the droplet and A_{tot} is the total mass of the system (droplet plus vapor) and a strict mass conservation has been implemented. If we introduce the vapor fraction $x = 1 - A/A_{tot}$ and the reduced temperature $\tau = T/\Delta e_0$, the relation between τ and x (which is monotonically correlated to the energy) at constant volume can be written as

$$c_1 - \frac{1}{\tau} + \frac{c_2}{\tau(1-x)A_{tot}^{1/3}} = \ln \tau + \ln \frac{x}{1 - c_3(1-x)}. \quad (12)$$

Here, $c_1 = \ln(p_0/\rho\Delta e_0)$, $c_2 = 3a_s v_l / r_0 \Delta e_0$, $c_3 = \rho v_l$ contain the specific features of the physical system under study and are linked to its bulk pressure, surface properties and the system volume, respectively. In the thermodynamic limit $A_{tot} \rightarrow \infty$, the relation (12) between the temperature and the vapor fraction (i.e., the caloric curve) is monotonic in the physical domain $0 < x < 1$ for all physical values of the constants as expected. For finite systems, the equation of state can present a backbending with an amplitude depending on the value of the parameters c_1, c_2, c_3 . An example is given in Fig. 11 for $c_1 = 1$, and $c_2 = 0.25$, $c_3 = 0.1$. The quantity c_1 represents a global shift and does not influence the monotonic character of the equation of state. The quantity c_2 gov-

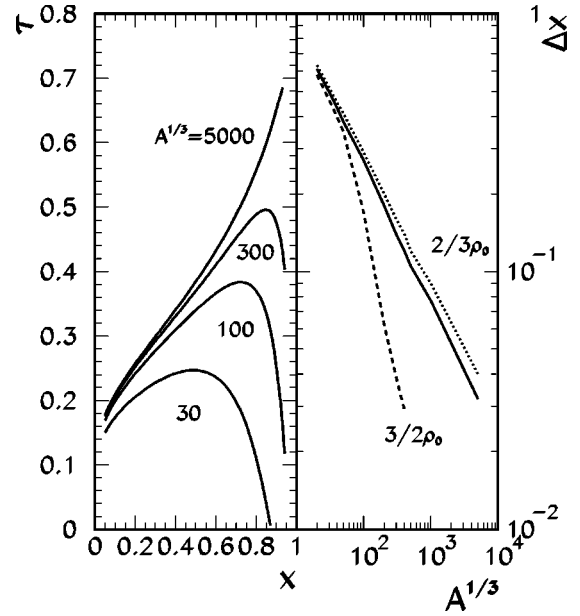


FIG. 11. Equation of state of a liquid droplet in equilibrium with its vapor from Eq. (12). Left side: reduced temperature as a function of the vapor fraction for different sizes of the system. Right side: vapor fraction interval of the negative heat capacity region as a function of the size of the system. Full line: same total density as in the calculation of the left panel; dashed (dotted) line: higher (lower) density.

erns the speed of convergence towards the thermodynamic limit, while the influence of c_3 is shown in the right part for Fig. 11. The backbending progressively decreases with the increasing size of the system but this phenomenon is not specific of very small droplets only. In order to quantify the evolution towards the thermodynamic limit, one may study the variation of the extension of the backbending region with the size of the system. To this aim, we have represented the vapor fraction interval corresponding to the slope inversion of the equation of state in the right part of Fig. 11. The monotonous correlation between the energy and the vapor fraction assures that the backbending in x corresponds to a backbending in energy, i.e., the adimensional quantity Δx is directly correlated to the energy jump in the backbending region. The clear power-law behavior as a function of the total mass of the system shows that the energy jump goes to zero only at the thermodynamic limit.

VI. CONCLUSIONS

In this paper, we have analyzed the different effects due to the finite size of the systems on the determination of order parameters and on the definition and classification of phase transitions using the Ising model with the fixed magnetization. A detailed comparison with the standard Ising model at zero field has shown the general effect of constraints on the equations of state of finite systems. Indeed, ensembles are, in general, not equivalent in finite systems and, in particular, first-order phase transitions manifest themselves in a very different way in the ensemble in which a constraint is put on the order parameter or on an observable closely connected to

it [24]. If we consider an ensemble in which a constraint is put on the order parameter, the bimodality in the order parameter distribution reflects as a backbending in the equation of state which links the order parameter to its associated intensive variable. Looking at the global topology of events in the observables space [16], we have shown that the first-order character of the transition also manifests itself even in lattice sizes as small as $L=6$ through bimodalities in variables only loosely connected to the magnetization. The connection between the event topology and the cluster distribution led to the conclusion that the apparent signs of a continuous transition seen in this model for small lattice sizes [2,10,15] can be interpreted as a finite-size effect. Indeed, fluctuations around the transition temperature can lead to an anomalously wide cluster distribution with an apparent power-law behavior and eventually a bimodality in the distribution of the largest connected domain. Because of the

correlation between the cluster sizes and the total energy, we have suggested that the anomalous backbendings observed in the caloric curve for very large lattices [13] are due to the same finite-size effects, and should disappear in the thermodynamic limit as expected from the Van Hove theorem. These speculations are comforted by the analytical study of a macroscopic liquid droplet in equilibrium with its vapor in a low density and low temperature approximation. The equation of state at constant volume presents a backbending in the coexistence region with an energy jump which decreases as a power law towards the thermodynamic limit.

ACKNOWLEDGMENTS

We thank A. Tarancón for many and very useful discussions. This work was partially supported by Spanish MCyT research contract no. FPA2001-1813.

-
- [1] S. Grossmann and W. Rosenhauer, *Z. Phys.* **207**, 138 (1967); P. Borrmann *et al.*, *Phys. Rev. Lett.* **84**, 3511 (2000); O. Mülken, H. Stamerjohanns, and P. Borrmann, *Phys. Rev. E* **64**, 047105 (2001).
- [2] F. Gulminelli and Ph. Chomaz, *Phys. Rev. Lett.* **82**, 1402 (1999); *Int. J. Mod. Phys. E* **8**, 527 (1999); R.M. Lynden-Bell and D.J. Wales, *J. Chem. Phys.* **101**, 1460 (1994).
- [3] D.H.E. Gross, *Phys. Rep.* **279**, 119 (1997); *Microcanonical Thermodynamics: Phase Transitions in Finite Systems*, Lecture Notes in Physics (World Scientific Singapore, 2001).
- [4] Ph. Chomaz, V. Dufloy, and F. Gulminelli, *Phys. Rev. Lett.* **85**, 3587 (2000).
- [5] J. Barré, D. Mukamel, and S. Ruffo, *Phys. Rev. Lett.* **87**, 030601 (2001).
- [6] E.G.D. Cohen, e-print cond-mat/0101311.
- [7] M. D'Agostino *et al.*, *Phys. Lett. B* **473**, 219 (2000); *Nucl. Phys. A* **699**, 795 (2002).
- [8] M. Schmidt *et al.*, *Phys. Rev. Lett.* **86**, 1191 (2001); **87**, 203402 (2001).
- [9] F. Gobet *et al.*, *Phys. Rev. Lett.* **89**, 183403 (2002).
- [10] J.M. Carmona, N. Michel, J. Richert, and P. Wagner, *Phys. Rev. C* **61**, 037304 (2000).
- [11] N. Fusco and M. Zannetti, e-print cond-mat/0210502.
- [12] T.L. Hill, *Thermodynamics of Small Systems* (Dover Publications, New York, 2002).
- [13] M. Pleimling and A. Hueller, *J. Stat. Phys.* **104**, 971 (2001).
- [14] M. Kastner, *J. Stat. Phys.* **109**, 133 (2002).
- [15] J.M. Carmona, J. Richert, and P. Wagner, *Phys. Lett. B* **531**, 71 (2002).
- [16] Ph. Chomaz, F. Gulminelli, and V. Dufloy, *Phys. Rev. E* **64**, 046114 (2001).
- [17] M.S.S. Challa *et al.*, *Phys. Rev. B* **34**, 1841 (1986); K.C. Lee, *Phys. Rev. E* **53**, 6558 (1996); Ph. Chomaz and F. Gulminelli, *Physica A* (to be published), e-print cond-mat/0210456.
- [18] J.M. Carmona, J. Richert, and A. Tarancón, *Nucl. Phys. A* **643**, 115 (1998).
- [19] K. Binder and D.P. Landau, *Phys. Rev. B* **30**, 1477 (1984).
- [20] L. Van Hove, *Physica (Amsterdam)* **15**, 951 (1949); C.N. Yang and T.D. Lee, *Phys. Rev.* **87**, 404 (1952); K. Huang, *Statistical Mechanics* (Wiley, New York, 1963), Chap. 15.2, Appendix C.
- [21] A. Coniglio and W. Klein, *J. Phys. A* **13**, 2775 (1980).
- [22] X. Campi, H. Krivine, and A. Puente, *Physica A* **262**, 328 (1999).
- [23] R.M. Lynden-Bell, *Mol. Phys.* **86**, 1353 (1995).
- [24] F. Gulminelli and Ph. Chomaz, *Phys. Rev. E* **66**, 046108 (2002).
- [25] F. Calvo, *Ann. Phys. (Paris)* **24**, 4 (1999).
- [26] A.M. Ferrenberg and R.H. Swendsen, *Phys. Rev. Lett.* **61**, 2635 (1988).
- [27] H. Reiss, J.L. Katz, and E.R. Cohen, *J. Chem. Phys.* **48**, 5553 (1968); L.G. Moretto *et al.*, e-print nucl-th/0012037; e-print nucl-th/0208024.
- [28] S.K. Ma, *Statistical Mechanics* (World Scientific, Singapore, 1985), Chap. 15.
- [29] The values of the magnetization between the two peaks of the probability distribution are strongly suppressed (see Fig. 1), and this suppression increases with the size of the system. This means that in practical simulations of large lattices, the correspondence between Ising and IMFM breaks down and Eq. (4) is no longer an efficient method to calculate the thermodynamic properties of IMFM.